Reports

Melting Inhibition and Superheating of Ice by an Antifreeze Glycopeptide

C. A. Knight and A. L. DeVries

The melting of pure ice single crystals can be inhibited by the presence of an antifreeze glycopeptide isolated from an Antarctic fish. This inhibition effect exhibits crystallographic dependence and can result in superheating of the crystal by heat conduction across the ice-solution interface. The antifreeze molecules inhibit melting in a manner more or less symmetrical to their well-known effect of inhibiting freezing. The melting effect is best expressed at concave ice interfaces, whereas the freezing effect is best expressed at convex ones. Both are restricted to orientations near $(10\bar{1}0)$ with the particular antifreeze that was used.

Some fish that live in seawater at its freezing point produce a novel kind of antifreeze, water-soluble peptides or glycopeptides that prevent ice crystal growth but do not substantially lower the equilibrium freezing point of the water (or solution) in which they are dissolved. The antifreeze material used in this work was refined from the blood of the Antarctic fish *Dissostichus mawsoni*, which contains a mixture of eight glycopeptides (AFGPs) that differ from each other only in length. We used a mixture of **1** through **5** (molecular weight 33,700 to 10,500, **5** being the heaviest) (*1*). The "pure" water was filtered through several ion exchange filters and had a resistivity of 17 to 18 MΩ cm.

The experimental apparatus is sketched in Fig. 1. A single crystal of pure ice (grown from the pure water) with a vertical hole drilled into it from the top is supported inside an insulated box, itself within a chamber maintained at about +1°C, for several hours until melting starts and all material is at or above 0°C. A few tenths of a milliliter of either 2% by weight AFGP solution or pure water, initially at the experimental chamber temperature of +1°C, was placed in the hole, and an aluminum rod was inserted into the liquid so as to conduct heat from the outside and enlarge the hole by melting. The average molecular weight of the AFGP is about 20,000, and 2% by weight in solution depresses the equilibrium freezing point less than 0.1°C, whereas it reduces the ice crystal growth rate to zero in otherwise pure water at values of supercooling to −1.2°C (*1*).

The apparatus was designed to detect any anisotropy of melting rate, by inspection of horizontal cross sections of the hole after slow melting had proceeded for awhile. The heat flow is complicated in a vertical section but would be symmetrical in a horizontal section if melting were independent of the crystal orientation. The *D. mawsoni* AFGP has strong orientation-dependent effects upon crystal growth (*2*), and any such influence upon melting would be expressed by an asymmetry of the melted hole.

Four horizontal cross sections perpendicular to the hole axis, as sketched from photographs, but slightly idealized for the sake of illustration, are shown in Fig. 2, and examples are shown in Fig. 3. Two of the four cases in Fig. 2 had pure water in the hole and two had the AFGP solution, 2% by weight at the onset of melting. For each liquid, one case had the hole parallel to [0001] and the other perpendicular, as indicated (2% by weight was used because it produces nearly the maximum freezing inhibition effect). A basal facet, (0001), develops in the pure system, as do traces of prism faces. Since only basal faces have been reported in the slow growth of ice from pure water (*3*, *4*), traces of unwanted impurities may account for the prism face development. That these faces are striated (Fig. 3A) heightens this suspicion. The important point is the great effect of the AFGP upon melting, that is, strongly inhibiting it perpendicular to [0001] and especially at orientations near the prism plane. The melting interface texture is also illustrated in Fig. 3; generally smooth with pure water and very rough and faceted at a small scale with the AFGP.

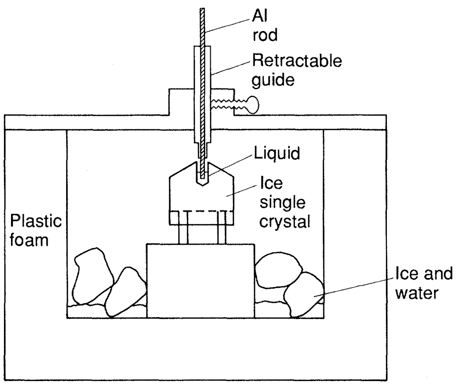

Fig. 1. The melting apparatus described in the text. The ice single crystal, about 3 cm by 4 cm by 5 cm, is supported by four short lengths of plastic drinking straw that rest against a layer of mosquito netting within the ice. Some such arrangement is needed to keep the ice, which melts on all sides, from moving. The drilled hole is 5.2 mm in diameter. The aluminum rod is 3 mm in diameter and is sheathed in teflon near the tip. The top of the ice is tapered to keep as much of the surface melt water as possible from running into the hole. A retractable guide is used for centering the rod in the hole.

Since the initial heat flow is identical in all of the experiments, in the ones with AFGP the ice must become appreciably superheated near the interfaces where the melting is retarded. However, the superheating is

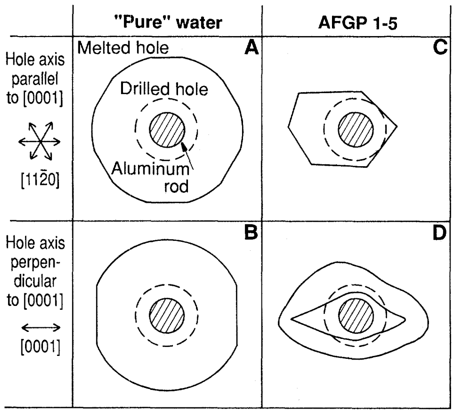

Fig. 2. Hole cross sections sketched from photos, but somewhat schematic, for the four cases: (**A** and **B**) "pure" water and (**C** and **D**) 2% by weight AFGP 1–5 (this solution becomes diluted with two to four times as much pure water during melting). In (A) and (C) the hole axis is parallel to [0001], and in (B) and (D) the axis is perpendicular to [0001]. External chamber temperature was +0.8° ± 0.1°C and the times varied from 20 to 30 hours. The 3-mm rod location is crosshatched and provides the scale, and the dashed circle is the original, drilled hole. In the absence of crystallographic effects upon melting, all of the hole cross sections would be circular because of the symmetry of the heat flow. For the AFGP case, with the hole axis normal to [0001], two cross sections are drawn, the inner one below the end of the original drilled hole. A side view of this is shown in Fig. 3B. Some of the facets in (C) are distinctly off the $(10\bar{1}0)$ orientation, which probably relates to evidence that the adsorption plane is actually a rather high-index plane near $(10\bar{1}0)$—perhaps $(72\bar{9}0)$ (*12*).

C. A. Knight, National Center for Atmospheric Research, Boulder, CO 80307.
A. L. DeVries, Department of Physiology and Biophysics, University of Illinois, Urbana, IL 61801.

more strikingly illustrated by Fig. 4, in which 2% AFGP was used, with the hole axis parallel to [0001] in an ice crystal that contained some small air bubbles that had been included during growth (ice free of air bubbles was selected for most of the experiments). The view in Fig. 4 is through the ice looking from beneath at the melted hole after it was emptied of the AFGP solution. Note the arms extending to the right and left, two of which to the left terminate at air bubbles about 1 mm in diameter. These arms have a grayish hue, and most of them contain a central line of small elongated air bubbles. When the main hole was drained, AFGP solution within these arms was retained by capillary forces and then frozen solid in the cold room (−15°C) where the photos were taken.

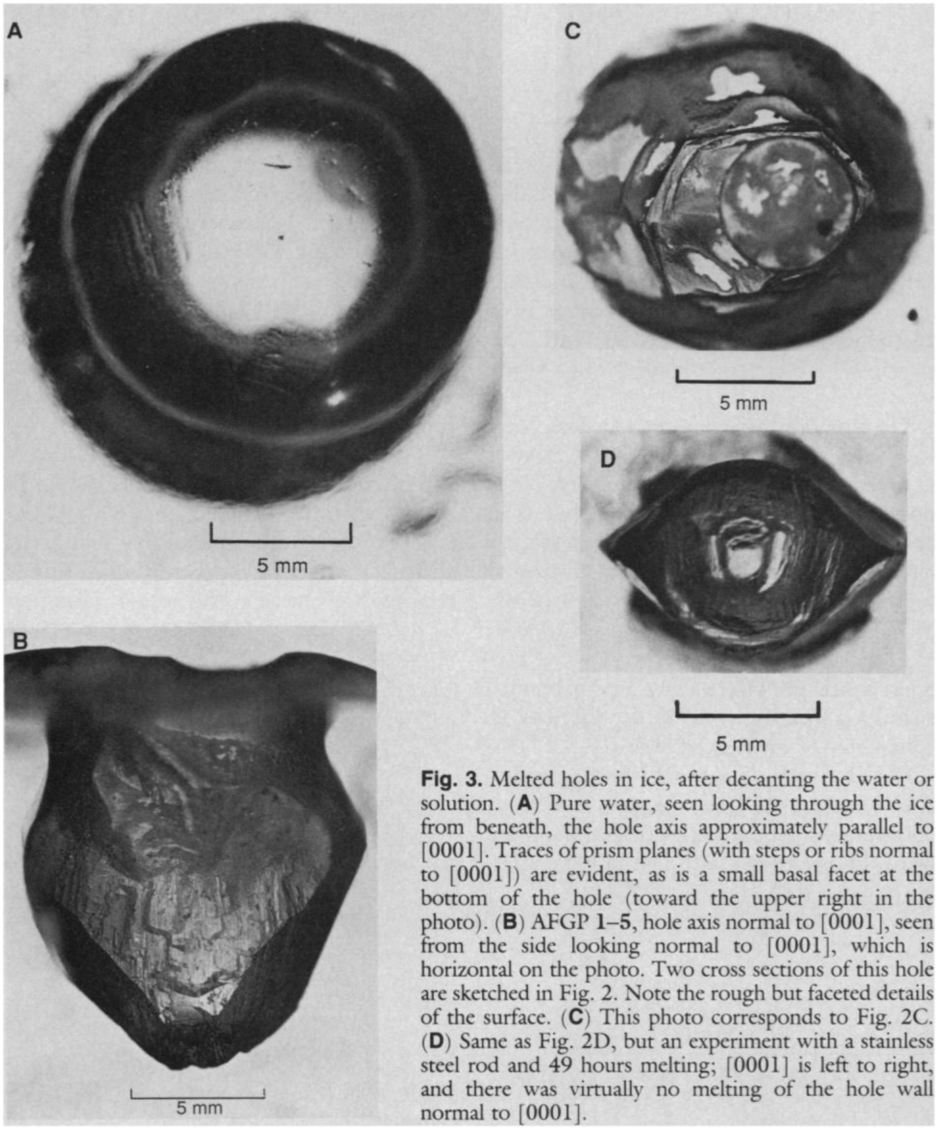

Fig. 3. Melted holes in ice, after decanting the water or solution. (**A**) Pure water, seen looking through the ice from beneath, the hole axis approximately parallel to [0001]. Traces of prism planes (with steps or ribs normal to [0001]) are evident, as is a small basal facet at the bottom of the hole (toward the upper right in the photo). (**B**) AFGP 1–5, hole axis normal to [0001], seen from the side looking normal to [0001], which is horizontal on the photo. Two cross sections of this hole are sketched in Fig. 2. Note the rough but faceted details of the surface. (**C**) This photo corresponds to Fig. 2C. (**D**) Same as Fig. 2D, but an experiment with a stainless steel rod and 49 hours melting; [0001] is left to right, and there was virtually no melting of the hole wall normal to [0001].

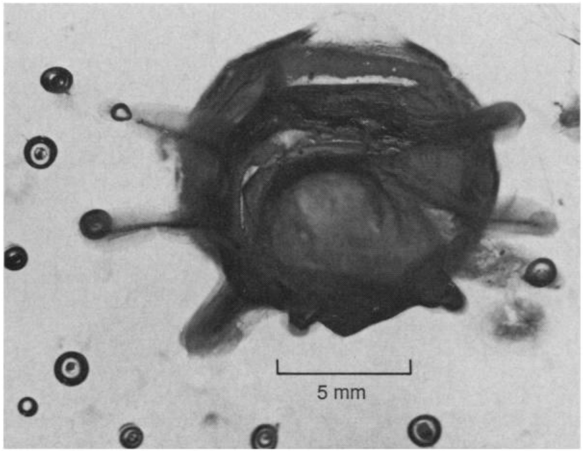

Fig. 4. Melted hole, axis parallel to [0001], decanted, seen from below, AFGP case. The hole is quite irregular, with arms extending out to preexisting air bubbles in the ice. The ice superheated in the vicinity of the hole, causing melting starting at the air bubbles and tunneling back to the hole. In most cases the air bubbles themselves are no longer present, but two prominent ones remain at the left side of the hole and about 5 mm from it.

Melting started at these air bubbles, several millimeters from the drilled hole containing the heat source (the aluminum rod), and "tunneled" back toward the drilled hole. This result confirms the presence of a temperature gradient, which demonstrates that superheating occurred that was maximal at the interface between the AFGP solution and the ice. When each channel reached the hole, the AFGP diffused into it, and the features of Fig. 4 resulted. Another experiment that showed the same effect was to drill the hole for melting near one side of the ice crystal. If [0001] is parallel to that side, the ice crystal just adjacent to the hole then melts inward much faster than elsewhere, leaving a hollow adjacent to the hole.

It appears that the strength of the melting inhibition effect may approach that of the freezing inhibition effect, although lacking a way to measure ice temperatures above 0°C, it would be much more difficult to quantify. Contact with any known physical sensor initiates melting and relieves the superheating. Although superheating of ice has been studied [see, for example, (*5*)], appreciable superheating of ice (or any pure crystal) by simple heat conduction, without using radiation or manipulating pressure, may not have been published previously (*6*).

Crystal growth typically deals only with interfaces that are convex toward the growth medium, and it is a basic geometrical understanding that faces develop normal to the slow-growth directions of the crystals. (Visualize a single crystal sphere with a zero growth rate due north and non-zero growth rates at other orientations. The crystal grows up to the plane tangent at the north pole and makes a facet.) Once this is understood, it is clear that in crystal growth at a concave surface, any face development would be normal to a fast-growth direction. Likewise, in crystal melting at a concave surface, any face development is normal to a slow-melting direction (*7*). This melting geometry is analogous to ordinary crystal growth in terms of expected shape development, and this was the reason for the melting-in-a-hole design of the experiment. These considerations explain why superheating has not been observed in many previous examinations of the freezing hysteresis: a convex crystal can melt completely with the melting occurring only at surfaces oriented at or near (0001), where adsorption does not retard the melting rate. It also provides an explana-

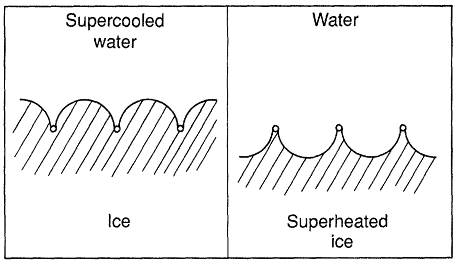

Fig. 5. Simple model of melting and freezing inhibition operating through the Kelvin effect—the influence of surface curvature upon melting point. The local radius of curvature needed to shift the melting point up or down by 1°C is about 175 Å if the surface energy is taken to be 20 ergs cm^{-2} and the geometry is idealized as two dimensional. The third dimension is important in the real case.

tion of the characteristics of the growth pits on the basal face of ice that form during growth within the freezing hysteresis gap (*8*). As far as the pits are concerned, this is freezing at a concave ice surface.

The mechanism of action of AFGPs and AFPs (antifreeze peptides) is under active study at present (*1*, *9–11*), and it is of interest that one of them inhibits melting in a way at least roughly symmetrical to its freezing inhibition. Probably the others do as well, although many of them may adsorb preferentially at interface orientations different from that of *D. mawsoni* (*12*). One can imagine two ways in which the AF molecules can adhere tightly enough to the ice-water interface to prevent growth or melting. One is ordinary adsorption, in which the linear or helical (*11*) molecules lie flat on the surface and bond to the ice, presumably fitting the ice surface structure (*1*), and the other would require some ice growth to engulf part of an AF molecule inside the ice crystal itself. Further ice growth might then be inhibited if there is a high free energy barrier against the rest of the molecule becoming buried within the crystal. These melting inhibition results argue against the need for partial engulfment and support of the idea of ordinary adsorption and the use of the phrase "adsorption inhibition" (*2*) for the antifreeze effect. (In fact, deciding this issue was the original motivation for this work.)

A two-dimensional representation of a simple, hypothetical mechanism for both freezing and melting inhibition by adsorption is shown in Fig. 5. It requires the adsorbed molecules to be bonded onto the ice-water interface very tightly and operates through the Kelvin effect. During either melting or freezing, the interface has to assume a radius of curvature before it can move past the originally adsorbed molecules and leave them completely within the liquid or the crystal. This radius of curvature dictates the supercooling or superheating required for motion of such an interface. The original hypothesis for freezing inhibition (*2*) involved the adsorbed molecules interfering with step passage, and is also, in principle, applicable to melting.

REFERENCES AND NOTES

1. A. L. DeVries, *Philos. Trans. R. Soc. London Ser. B* **304**, 165 (1984).
2. J. A. Raymond and A. L. DeVries, *Proc. Natl. Acad. Sci. U.S.A.* **74**, 2589 (1977).
3. W. B. Hillig, in *Growth and Perfection of Crystals*, R. H. Doremus, B. W. Roberts, D. Turnbull, Eds. (Wiley, New York, 1958), pp. 349–359.
4. C. A. Knight, *Nature* **220**, 62 (1968).
5. B. Kamb, *Science* **169**, 1343 (1970).
6. We learn from F. C. Frank that he was shown a demonstration of crystal superheating by G. Sears. Heat was fed into a flat face of a thin, perfect crystal—probably of salol—and melting occurred only at the edges.
7. F. C. Frank, in *Growth and Perfection of Crystals*, R. H. Doremus, B. W. Roberts, D. Turnbull, Eds. (Wiley, New York, 1958), pp. 411–418; F. C. Frank, *Z. Phys. Chem. Neue Folge* **77**, 84 (1972); C. A. Knight and N. C. Knight, *Science* **150**, 1819 (1965); C. A. Knight, *J. Appl. Meteorol.* **5**, 710 (1966).
8. J. A. Raymond, P. Wilson, A. L. DeVries, *Proc. Natl. Acad. Sci. U.S.A.* **86**, 881 (1989).
9. A. L. DeVries, in *Animals and Environmental Fitness*, R. Gilles, Ed. (Pergamon, Oxford, 1980), pp. 583–607.
10. R. E. Feeney and Y. Yeh, *Adv. Protein Chem.* **32**, 191 (1978).
11. D. S. C. Yang, *et al.*, *Nature* **333**, 232 (1988).
12. C. A. Knight and A. L. DeVries, in *Atmospheric Aerosols and Nucleation*, P. E. Wagner and G. Vali, Eds. (Springer-Verlag, Berlin, 1988), pp. 717–720. Our unpublished work suggests that the adsorption plane for *D. mawsoni* AFGP is a high-index one near the prism plane, $(72\bar{9}0)$.
13. We thank C. DeVries for helpful criticism of the manuscript. The National Center for Atmospheric Research is sponsored by the National Science Foundation. Supported in part under NSF DPP grant 87-16296 to A.L.D.

20 March 1989; accepted 8 June 1989

Disorder-to-Order Transition in Settling Suspensions of Colloidal Silica: X-ray Measurements

K. E. DAVIS, W. B. RUSSEL, W. J. GLANTSCHNIG

Dispersions of colloidal particles exhibit thermodynamic properties similar to those of molecular systems, including a hard sphere disorder-to-order transition. In experiments with organophilic silica in cyclohexane, gravity settling was used to concentrate the particles. With small particles the slow sedimentation permits rearrangement into the iridescent ordered phase, but larger particles form amorphous sediments instead. Scanning electron microscopy of the crystalline sediment indicates hexagonally close-packed layers. X-ray attenuation measurements reveal a discontinuity coincident with the observed boundary between iridescent and opaque regions. Sediments accumulating faster than the maximum rate of crystallization produce a glass, in accord with the classical theory for crystal growth.

SEDIMENTATION PROVIDES A MECHANISM for concentrating a dilute dispersion, forming a dense sediment on the bottom and clear liquid above. However, colloidal particles also execute Brownian motion and hence share many dynamic and thermodynamic properties with molecular systems, except with much longer relaxation times. For example, colloids diffuse down gradients in chemical potential and exhibit disorder-to-order transitions at high solid volume fractions. Thus the nominally simple sedimentation process actually couples gravity settling, diffusion, and crystallization in a highly nonideal system.

For hard spheres, the simplest of systems, short-range correlations characterize the disordered fluid state at volume fractions $\phi < 0.50$. However, both molecular dynamics simulations (*1*) and density functional theories (*2*) predict an ordered equilibrium state at higher volume fractions. Thus a hard sphere system at $\phi > 0.50$ should rearrange spontaneously, as a result of Brownian motion, from an initially disordered state into the equilibrium ordered state.

Indeed, Hachisu and Kobayashi (*3*) detected coexisting disordered and ordered phases, with $\phi = 0.50$ and 0.55, respectively, for aqueous polymer lattices at ionic strengths high enough to screen electrostatic repulsions. Recently, Pusey and van Megen (*4*, *5*) observed the transition for polymethylmethacrylate spheres at $0.56 > \phi \geq 0.50$ in a nonaqueous solvent but glasses at higher ϕ where the low mobility of the spheres apparently suppresses the rearrangement (*6*). Our experiments were designed to monitor crystallization during sedimentation and thereby provide information on the dynamics of the crystallization process.

K. E. Davis and W. B. Russel, Department of Chemical Engineering, Princeton University, Princeton, NJ 08544.
W. J. Glantschnig, AT&T Engineering Research Center, Post Office Box 900, Princeton, NJ 08540.